Molecular Structure in the Crystalline Phase of a Segmented Liquid Crystalline Polyester

ARTICLE · NOVEMBER 2000

DOI: 10.1021/ma0012346

4 AUTHORS, INCLUDING:

Domenico Acierno

University of Naples Federico II

341 PUBLICATIONS **3,481** CITATIONS

SEE PROFILE

Simona Concilio

Università degli Studi di Salerno

53 PUBLICATIONS **528** CITATIONS

SEE PROFILE

Paolo Vacca

SAES Getters Group

33 PUBLICATIONS **629** CITATIONS

SEE PROFILE

Molecular Structure in the Crystalline Phase of a Segmented Liquid Crystalline Polyester

Domenico Acierno,[†] Simona Concilio,[‡] Pio Iannelli,*[,‡] and Paolo Vacca[‡]

Dipartimento di Ingegneria dei Materiali e della Produzione, Università di Napoli, P.le Tecchio, I-80125 Napoli, Italy and Dipartimento di Ingegneria Chimica ed Alimentare, Università di Salerno, via Ponte Don Melillo, I-84084 Fisciano (Salerno), Italy

Received July 17, 2000; Revised Manuscript Received September 26, 2000

ABSTRACT: Molecular structure refinement of a liquid crystalline segmented polymer using X-ray diffraction methods is reported. The investigated polymer contains the 3-allylbiphenyl unit as nematogenic unit. The space group is $P2_1/a$, with cell parameters $a = 12.82$ Å, $b = 8.44$ Å, $c = 19.72$ Å, and $\beta = 153.2°$, with two chains per unit cell. The main feature of this molecular packing is the layered organization of chains with a transversal intercalation of the flexible and the rigid units in the layer. Repetition of layers in space leads to an herringbone packing of biphenyl units along [001]. Transversal register between chains is such that the two phenyl rings of biphenyl unit are involved in "edge to face" contact.

Introduction

Liquid crystalline polymers (LCPs) have been largely investigated for their unique properties, being confined between the crystalline-ordered and the liquid-disordered states. Liquid crystalline order is characterized by a large number of molecular organizations which have been described and classified by several authors and are mainly based on investigations carried out on low molecular weight LC compounds.[1,2] Since LCPs were discovered, a lot of work has been done in order to extend the structural classification of LC order to LCPs, taking into account the defective structure of high molecular weight compounds.[3−5]

A basic "ingredient" for synthesizing PCLs is a molecular frame having adequate elongation (high "axial ratio") and rigid conformation.[6] Axial ratio is defined as the ratio between the length and the width of a cylinder that ideally reproduce the overall shape of the molecular frame. Of course, this "cylinder" may be rigid to partially flexible as well as linear or bent depending on the chemical structure. The accommodation of this molecular frame in the condensed state brings to numerous LC structures[3−5] ranging, for example, from the less ordered nematic phase to the highly structured smectic S_F and S_I. In the case of main-chain LCPs, molecular frames with high axial ratio are attached each other along the chain both with and without intercalation of flexible spacers, such as for instance an aliphatic unit. In this way the two classes of rigid rod (RLCPs) and segmented (SLCPs) liquid crystalline polymers are obtained, respectively. In the latter case, the length and the architecture of the flexible unit also contribute to set the physical properties of polymers.

Recently, we have reported on a class of SLCPs with formula[7,8]

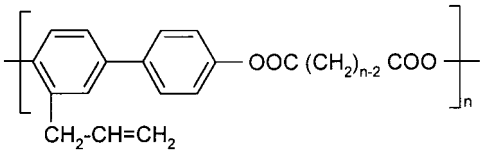

P(n) n=6,8,10,12,14

in order to study the effect of cross-linking of allyl group on mesophasic and tensile performance of polymers. **P(*n*)** show a nematic phase with the isotropisation ranging from 90 °C to 175 °C, depending on the length of the flexible spacer.[7] At room temperature, **P(8)** shows a very well developed crystalline phase, while only a mesophasic order is observed for other polymers.[7] Such a singular difference prompted us to investigate on the correlation between chemical formula (in this case the number of methylene units in the chain) and molecular packing in order to find out an explanation for such a difference. For this purpose, we report in this paper on the synthesis of copolymers **P(8−*x*)** with formula

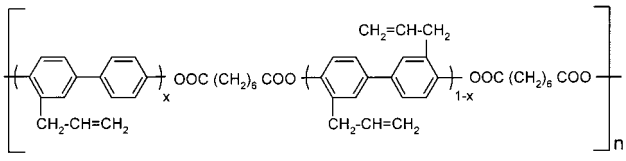

P(8-x) **x**=1, 0.80, 0.50, 0.20, 0

On the basis of structural change of **P(8−*x*)** as a function of composition *x*, we have performed X-ray diffraction analysis and molecular structure refinement of **P(8)** [≡**P(8−1)**] in the crystalline phase.

Experimental Section

Polymer Synthesis. All reagents were used as obtained from Aldrich. **P(8−*x*)** were synthesized by the interfacial polycondensation reaction of a mixture of 3-allyl-4,4′-dihydroxybiphenyl and 3,3′-diallyl-4,4′-dihydroxybiphenyl and the

* Corresponding author. E-mail: Iannelli@dica.unisa.it.
† Università di Napoli.
‡ Università di Salerno.

10.1021/ma0012346 CCC: $19.00
Published on Web 12/01/2000

Table 1. Data Concerning Virgin Samples of P(8−*x*) without Annealing (Melting and Isotropization Temperatures Measured at the Maximum of the Endothermic Transitions)

polymer	T_m[a]	ΔH_m[b]	T_i[c]	ΔH_i[d]	M_w ($\times 10^3$)
P(8)	119.2	15.1	140.8	15.1	145
P(8−0.8)	111.3	21.5	110.2[e]	7.9 [f]	27.4
P(8−0.5)	91.2	23.1	72.9[e]	12.2 [f]	35.0
P(8−0.2)	76.0	25.1			27.4
P(8−0)	73.6				34.9

[a] T_m /°C, melting temperature. [b] ΔH_m/Jg^{-1}, melting enthalpy. [c] T_i/°C, isotropization temperature. [d] ΔH_i/Jg^{-1}, isotropization enthalpy. [e] Anisotropization temperature, measured using the cooling trace. [f] Anisotropization enthalpy, measured using the cooling trace.

acid chloride of the appropriate α,ω-dicarboxy-*n*-alkane, as outlined in refs 7 and 9. Weight-averaged molecular weights by GPC are given in Table 1. Proton resonance data are in agreement with the standard values.

Characterization. Fiber samples of **P(8)**, **P(8−0.8)**, and **P(8−0.5)** were extruded from the nematic phase and cooled to room temperature. The average diameter of the fibers is 200−300 μm. For **P(8−0.2)** and **P(8−0)**, which do not show the nematic phase, film samples were prepared by casting from solution of polymers in chloroform (final thickness of about 100 μm). Polymer films were oriented by stretching at room temperature ($\lambda \approx 3-3.5$) to perform X-ray diffraction measurements

Thermal measurements were carried out by means of a DSC-7 Perkin-Elmer calorimeter under nitrogen flow at 10 °C/min rate.

Polarized optical microscopy was performed by means of a Jenapol microscope fitted with a Linkam THMS 600 hot stage.

Diffraction spectra were recorded under vacuum by means of a cylindrical camera with a radius of 57.3 mm and the X-ray beam direction perpendicular to the fiber axis (Ni-filtered Cu Kα radiation). High-temperature measurements were carried out by means of a flat camera equipped with a modified Linkam THMS 600 hot stage, with a sample to camera distance of 7.0 cm. The Fujifilm MS 2025 imaging plate and a Fuji Bioimaging analyzer System, model BAS-1800, were used for digitizing the diffraction patterns.

The ^{1}H NMR spectra were recorded in $CDCl_3$ solution with a Brucker DRX/400 spectrometer.

For GPC analysis a Waters 150-C ALC/GPC instrument was employed, equipped with six 300 × 7.5 mm^2 columns (types: Waters Styragel HT3, HT4, HT5, HT6, 500 Å, and 400 Å) and a Jasco 875 UV detector set at 254 nm (polystyrene as standard and chloroform as solvent, at 1 mL/min and 30 °C).

Structure Refinement Procedure. The "Whole Pattern" method [10−13] is employed to carry out the analysis and the refinement of the crystalline structure. The method applies the least-squares fitting procedure to obtain the best match between the two-dimensional experimental and calculated X-ray diffraction patterns.[11−13] To ensure the convergence of the fitting, it is necessary to have a reliable starting model of the molecular structure. Parameters to be refined are of two kinds: (i) nonstructural ones, like the crystalline size and the degree of crystallites orientation with respect to the fiber axis, and (ii) structural ones, like the torsion angles defining chain conformation. The former sets the shape, while the latter sets the diffraction intensity of each diffraction spot.

In this article, the nonstructural parameters are considered: (a) the main crystallite size [Δ*a*, Δ*b*, and Δ*c*] taken along a direction parallel to the lattice axes [*a*, *b*, and *c*, respectively]; (b) the averaged angle [α_0] between the *c* lattice axis of crystallites and fiber axis, where α_0 is related to the degree of fiber orientation; (c) the case where crystallites may be oriented along a direction that does not coincide with the fiber axis. In the present case crystallites are tilted preferentially around [010]. The angle of rotation, to be evaluated and refined, is named μ.

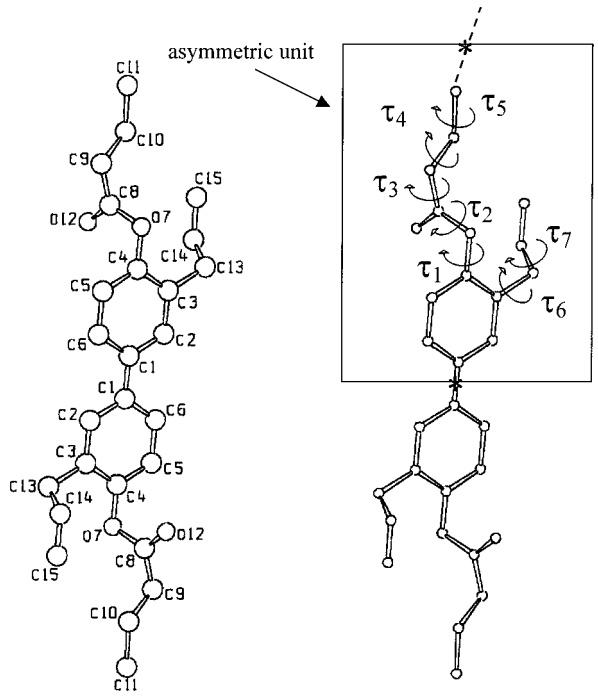

Figure 1. Chain representation: torsion angles τ_i are defined according to Table 5; centers of symmetry (∗) are placed in the middle of biphenyl and aliphatic units.

Table 2. *d*-Spacing (in Å) Correspondent to the Bragg Reflections in the Equatorial Line of Annealed Fiber Diffraction Spectra of P(8−*x*) (Intensity on a Visual Basis: vvs = Very Very Strong, vs = Very Strong, s = Strong, w = Weak)

hkl[a]	P(8)[b]		P(8−0.8)[c]		P(8−0.5)[d]		P(8−0.2)[e]		P(8−0)[f]	
									19.7	m
100									7.09	s
110	4.78	vvs	4.80	vvs	4.91	vs	5.19	vs	5.29	vs
									4.35	s
020	4.20	vs	4.21	vs	4.22	vs	4.18	s	4.06	vs
120	3.42	w	3.42	w	3.50	w			3.55	w
200	2.90	w	2.92	w	3.02	w				
220	2.39	w	2.40	w	2.46	w				

[a] Bragg indices only for **P(8)**, **P(8−0.8)**, and **P(8−0.5)**. [b] Diffraction pattern given in Figure 3b. [c] Diffraction pattern given in Figure 4a. [d] Diffraction pattern given in Figure 4b. [e] Diffraction pattern given in Figure 4c. [f] Diffraction pattern given in Figure 4d.

Table 3. Cell Parameters for P(8-*x*) (Obtained by the Best Fitting of the Strongest 10 Bragg Reflections in the Diffraction Pattern)

	a (Å)	*b* (Å)	*c* (Å)	α (deg)	β (deg)	γ (deg)
P(8)	12.82(1)	8.44(1)	19.72(1)	90	153.2(1)	90
P(8−0.8)	12.8(1)	8.44(3)	19.73(4)	90	152.8(3)	90
P(8−0.5)	13.0(1)	8.49(3)	19.72(5)	90	152.3(3)	90
P(8−0.2)	13.20(5)	8.41(5)	19.73(7)	90	150.0(4)	90
P(8−0)	14.9(3)	8.27(5)	19.73(6)	90	151.9(5)	90

The structural parameters to be refined are as follows: (a) lattice parameters defining the unit cell; (b) fractional coordinates of the center of mass of the chain (in our case only the z_0 coordinate according to the $P2_1/a$ space group), and the angle of rotation (Φ_0) of chain [Φ_0 is defined as the angle between two planes intersecting each other along a line connecting the two centers of symmetry of the chain, where one plane is parallel to (010) while the second one contains atom C3]; (c) torsion angles τ_i defining the chain conformation (Figure 1 and Table 5).

The following structural parameters are kept fixed during refinement: bond lengths C−C = 1.54 Å, aromatic C═C = 1.40

Table 4. Calculated Integrated Intensities of the Strongest Diffraction Spots as Obtained by the Structure Refinement of P(8)

hkl[a]	I_{calcd}[b]	hkl[a]	I_{calcd}[b]
110	100	111	17.0
020	57.0	001	0.5
120	3.6	1$\bar{1}$2	1.8
1$\bar{1}$1	2.9	2$\bar{0}$2	1.0
011	<0.1	2$\bar{1}$2	0.8
2$\bar{0}$1	2.5	002	<0.1
1$\bar{2}$1	8.4		

[a] Bragg indices. [b] Calculated integrated intensities I_{calcd} are normalized to the maximum intensity peak of 100. Intensity is not corrected for the Lorentz factor.

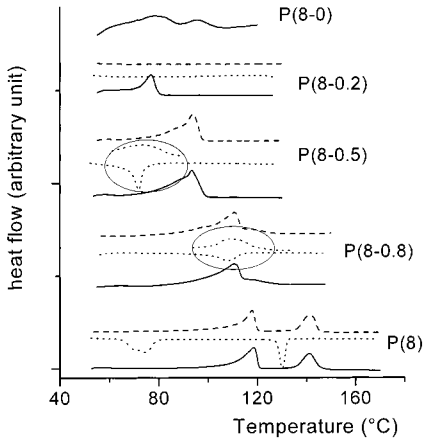

Figure 2. DSC traces of powder samples of **P(8−*x*)**: (−) first heating run; (····) first cooling run; (---) second heating run. For **P(8−0.8)** and **P(8−0.5)** the isotropization transition is visible as a small exothermic peak in an heating run performed quickly after the anisotropization (see in the ellipses).

Å, double bond C=C = 1.34 Å, C=O = 1.23 Å, C−O = 1.43 Å, C−H = 1.08 Å; bond angles O−C−C = 109.5°, C−O−C = 109.5°, O−CO−C = 120°, C−C=C = 120°, and aromatic C−C−C = 120°. The isotropic thermal parameter B_{iso} is refined to be equal for all atoms. Hydrogen atoms, placed using canonical sp^2 and sp^3 geometry, are included in the calculation. During refinement, a constraint is imposed to the chain backbone; i.e. the chain length must match the *c* axis length.

Discussion

Thermal and Preliminary X-ray Diffraction Characterization. P(8), P(8−0.8), and **P(8−0.5)** show the nematic phase according to the optical microscopy and the X-ray diffraction analysis [in the case of **P(8)**, the halo peaked at (sin θ)/λ = 0.11 Å^{-1} and no Bragg diffraction for lattice distances lower than about 41 Å was observed]. Thermodinamical data are given in Table 1 while DSC heating/cooling runs are shown in Figure 2. According to Figure 2, **P(8−0.8)** and **P(8−0.5)** are monotropic. In this case the isotropization transition is visible as a small exothermic peak in an heating run performed quickly after the anisotropization. **P(8−0.2)** and **P(8−0)** do not show LC order and only the solid-to-isotropic liquid and *vice versa* transitions are observed in the DSC traces. The X-ray diffraction patterns of annealed samples of **P(8−*x*)** are shown in Figures 3 and 4. In particular, the spectra of **P(8−*x*)** with $x = 1$, 0.8, and 0.5 are quite similar to each other while those for $x < 0.5$ are not. In terms of *d*-spacing, when *x* decreases the strong 110 equatorial reflection moves to lower angle (*d*-spacing increases) while the 020 reflection remains almost at the same angle, as seen in Table

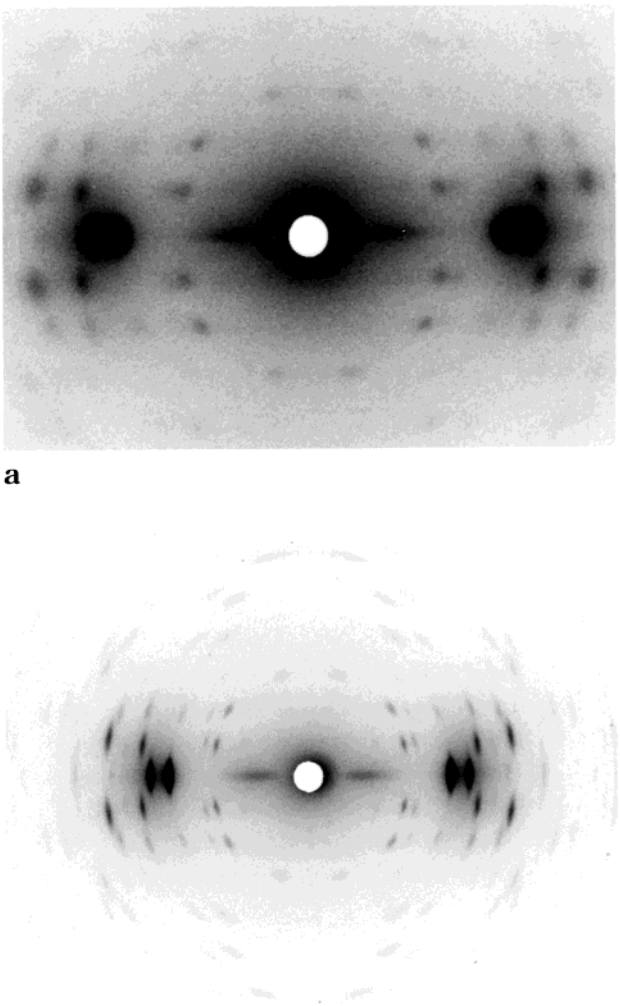

Figure 3. X-ray diffraction patterns of a virgin fiber sample of **P(8)**: (a) sample as extruded and (b) sample annealed at 110 °C for 2.5 h. Measurement taken at room temperature.

2 (see also the next section). Thus, increasing the content of the allyl unit enlarges the crystallographic axis *a*, which suggests a molecular packing of the allyl unit parallel to [100]. Moreover, the decrease of *x* gives rise to a less ordered molecular packing according to the few and less defined reflections in the diffraction pattern.

If we refer to the homopolymers series **P(*n*)**,[7] **P(8)** is the only crystalline polymer, as outlined in the Introduction section. **P(*n*)** with $n \neq 8$ are not crystalline and show only a mesophasic structure even after a prolonged annealing. For example, fiber patterns of **P(6)** and **P-(12)** are shown in Figure 5 to be compared to that of **P(8)** shown in Figure 3.

Krigbaum et al. showed that polymers with formula

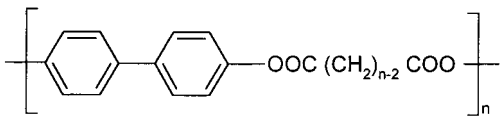

PW(n) n=8,10,12,14

are LCPs.[14,15] They reported that **PW(*n*)**s are crystalline materials melting to the smectic H phase, different from what we observed for **P(8−*x*)**; consequently, the allyl

Table 5. Parameters at the End of Structural Refinement with Standard Deviations in Parentheses

Structural Parameters			
$a = 12.82$ (1) Å	$b = 8.44$ (1) Å	$c = 19.72$ (2) Å	$\beta = 153.2$ (1)°
$\Phi_0 = 49$ (2)°			
$\tau_1 = -117.4$ (8)° [C3−C4−O7−C8]	$\tau_2 = 198.2$ (2)° [C4−O7−C8−C9]	$\tau_3 = -91$ (4)° [O7−C8−C9−C10]	$\tau_4 = -192$ (5)° [C8−C9−C10−C11]
$\tau_5 = 121.5$ (7)° [C9−C10−C11−C11*]	$\tau_6 = -106$ (10)° [C2−C3−C13−C14]	$\tau_7 = 244$ (9)° [C3−C13−C14−C15]	
Nonstructural Parameters			
$\Delta a = 179$ (4) Å	$\Delta b = 135.1$ (3) Å	$\Delta c = 153$ (3) Å	$\alpha_0 = 6.36$ (1)°
$\mu = 1.76$ (1)°	$B_{iso}{}^a = 7.4$ (1) Å^2		

[a] Isotropic thermal parameter, imposed to be the same for all atoms.

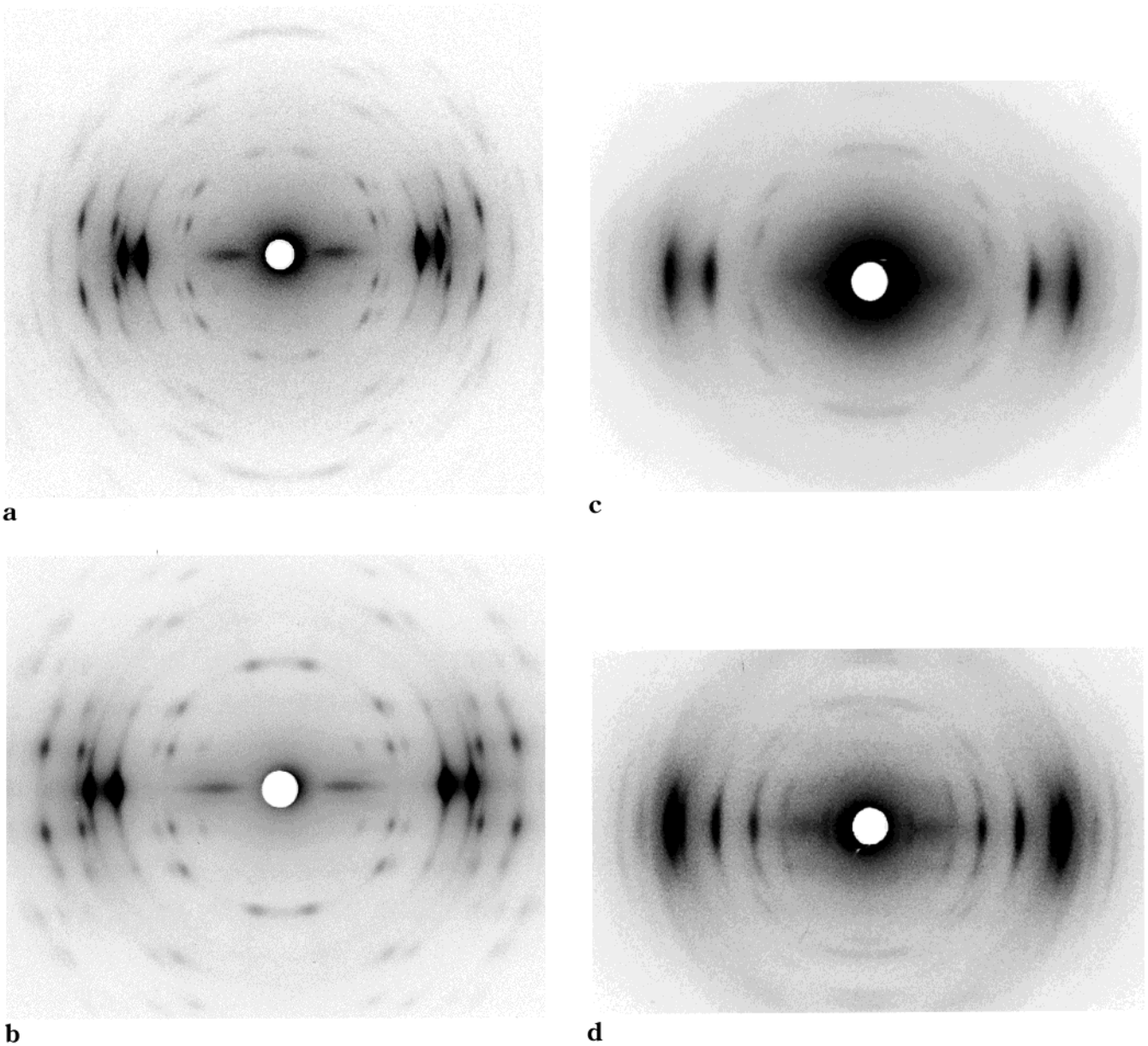

Figure 4. X-ray diffraction patterns of **P(8−*x*)**: (a) **P(8−0.8)** and (b) **P(8−0.5)** fiber samples; (c) **P(8−0.2)** and (d) **P(8−0)** film samples. Samples were annealed for 2.5 h at 95, 80, 60, and 60 °C, respectively. Measurements taken at room temperature.

unit deeply affects molecular packing, destabilizing both the crystalline and the high ordered H phases. The unique circumstance of a well developed crystalline order in the case of annealed samples of **P(8)** suggests that the allyl group, only in this case and for a reason to be understood, is compatible with a good molecular packing contrary to that observed for $n \neq 8$. As will be clarified by the structural refinement, the circumstance of an equal length of the flexible aliphatic and the rigid biphenyl units for **P(8)** leads to a tight molecular packing that is not allowed in the other cases.

Fiber Diffraction Spectra of P(8), Crystalline Phase. The main characteristic of the X-ray diffraction pattern of **P(8)** is the presence of numerous sharp diffraction spots. This circumstance brought us to hypothesize a large triclinic cell for the crystalline phase

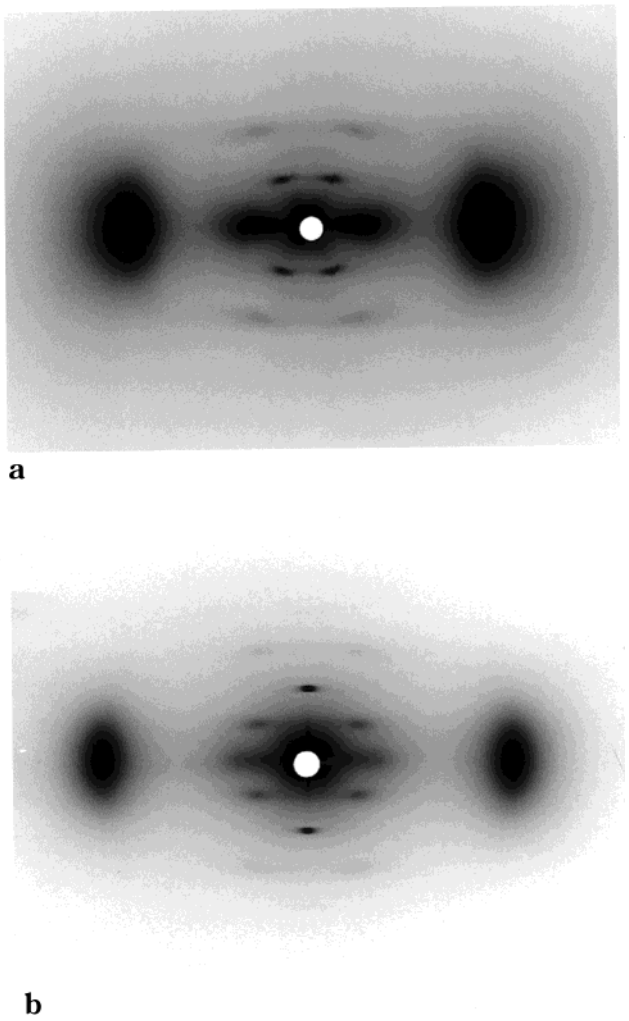

Figure 5. X-ray diffraction patterns of a virgin fiber sample of (a) **P(6)** and (b) **P(12)**. Measurement taken at room temperature.

of **P(8)** [$a = 9.62$ Å, $b = 8.92$ Å, $c = 20.2$ Å, $\alpha = 107.8°$, $\beta = 90.0°$, $\gamma = 81.0°$] with the anomalous occurrence of three chains per unit cell.[7] Indeed we expressed caution in assigning this unit cell because of the few diffraction spots in the equatorial line (five) compared to the layer lines: this suggests the presence of some extinction conditions incompatible with triclinic cell. To assign a new unit cell, we can take advantage of some differences in the diffraction patterns of **P(8−*x*)**. In particular, **P-(8−0)** shows a strong equatorial reflection with a spacing of 7.09 Å that is absent in the other cases. This spot may be extinct for **P(8)** because of a crystalline system with higher symmetry than the triclinic one, for instance the monoclinic system. In the hypothesis of a monoclinic system, the five detectable equatorial spots (Table 2) can be indexed as 110, 020, 120, 200, and 220 using a planar unit cell $a' = 5.80$ Å, $b' = 8.40$ Å, and $\gamma = 90°$. The evaluation of c axis and β angle (unique axis b) is quite difficult because of the slight but clearly detectable spreading of reflections out of the layer lines. This is due to the alignment of crystallites along a direction which is slight tilted respect to the fiber axis.[16] Indeed, the amount of tilting is small; thus, it can be evaluated directly in the refinement stage of molecular structure according to the general procedure.[11,12] In the hypothesis that the observed reflection on the first layer line close to the meridian has Bragg indices 001, the cell parameters evaluated by the best fitting of the 10 strongest reflections are $a = 12.8$ Å, $b = 8.4$ Å, $c = 19.8$ Å, and $\beta = 150°$, with two chains per unit cell. This cell reproduces all diffraction spots in the experimental pattern and will be used in the structure refinement stage. The clear absence of reflections $\bar{1}01/\bar{1}02$ and 100/010 restricts the choice to the space group $P2_1/a$. Because the two chains per unit cell and the four general positions for $P2_1/a$, the asymmetric unit must be half the monomeric unit. This is possible only by imposing a center of symmetry to the chain, coincident with the origin of unit cell, which may be placed reasonably at the center of mass of biphenyl unit and at the middle of aliphatic unit, as better discussed in the following. Lattice parameters of **P(8−*x*)** are given in Table 3.

P(8) Structure Refinement. The asymmetric unit of **P(8)** is depicted in Figure 1. The center of symmetry of biphenyl unit is placed at the origin of unit cell. In the first stage of the structure analysis, the most extended trans-planar conformation is imposed to the aliphatic unit and to the allyl group. This corresponds to having all torsion angles equal to 180° except τ_1, which is set to 60° to avoid intramolecular steric interactions. These constraints are removed stepwise in the refinement stage.

Because of the random insertion of the biphenyl unit along the chain due to the synthetic route, two allyl groups have to be taken into account, one for each of the two phenyl rings. Consequently an occupancy factor of 0.5 is imposed on the allyl unit, in agreement with the center of symmetry placed in the middle of the biphenyl unit.

Following the refinement procedure described in the Experimental Section, the convergence is reached stepwise. The observed and the calculated diffraction data at the end of the refinement are compared in Figures 6 and 7. Calculated integrated intensities for the strongest diffraction reflections are given in Table 4. Crystalline packing is shown in Figures 8−11. Refined parameters and atomic fractional coordinates are listed in Tables 5 and 6, respectively. All the intra- and intermolecular atomic distances are in agreement with the standard values excepted for the intermolecular short contact involving allyl groups that are not to be considered because their statistical nature. It is worth of note that, for this reason, the refined structure is not a "true one" but, strictly speaking, only the average of several structures involving different conformations or displacements of the allyl and biphenyl units. Each of these local structures are stereochemically consistent, but the averaged model, of course, is not.

Molecular packing is mainly characterized by a layered organization of chains. In fact the center of symmetry at the center of biphenyl unit, placed at the origin of unit cell, and the glide plane give rise to a layered packing of chains in the $x-z$ plane (Figure 11). The overall pseudohexagonal accommodation of chains into the layer is noteworthy. Looking at Figure 11, it is evident a face-centered register of chains changes into a little distorted rectangular frame having edges c and a'. Since

$$a' \approx 2\, a \sin\beta = 11.6 \text{ Å}$$

the condition $c/a' = \sqrt{3}$, required for a pseudohexagonal arrangement, is almost fulfilled ($c/a' = 1.706$ against the expected value of 1.732). The drawing force

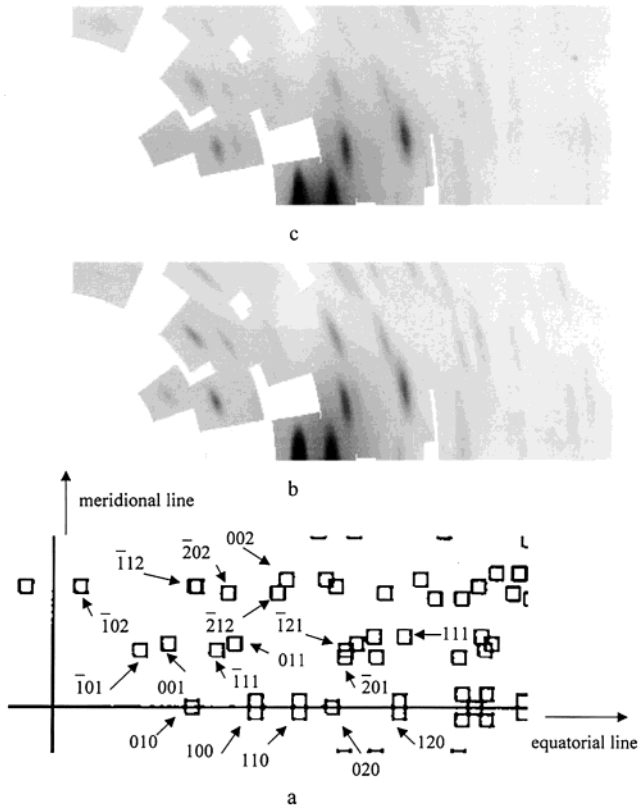

Figure 6. Two-dimensional representation of X-ray diffraction pattern of **P(8)** (crystalline phase): (a) schematic representation of diffraction pattern with Bragg indices of some reflections, including extinct ones; (b) calculated diffraction pattern according to this article; (c) observed diffraction pattern. The spreading of diffraction spots from the first layer line is evident. Only one of the four quadrants of the spectra is considered.

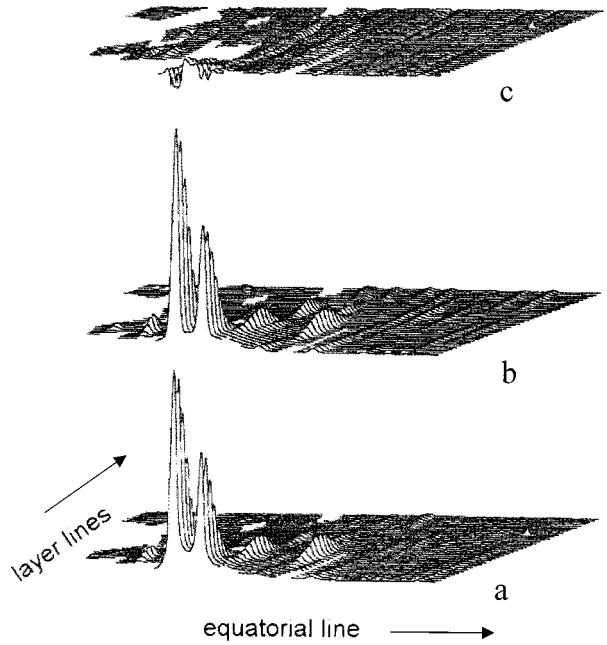

Figure 7. Three-dimensional representation of X-ray diffraction pattern of **P(8)** (crystalline phase, same date of Figure 6): (a) observed data; (b) calculated data according to this article; (c) the difference between parts a and b.

for this packing accommodation is the almost identical length of the two molecular frames along the chain (aliphatic and biphenyl units) that minimizes the steric

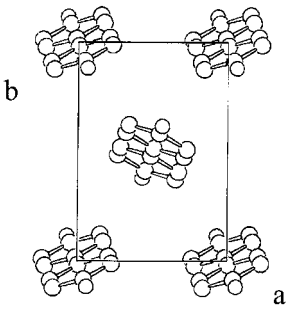

Figure 8. Molecular packing of **P(8)** viewed along the *c* axis [001]. For the sake of clarity only biphenyl units are drawn.

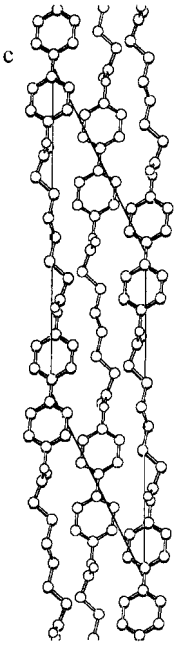

Figure 9. Molecular packing of **P(8)** viewed along the *b* axis [010].

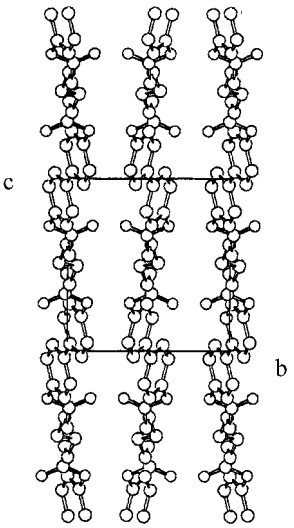

Figure 10. Molecular packing of **P(8)** viewed along the *a* axis [100].

interactions between adjacent rigid biphenyl moieties. This favorable circumstance is not possible for **P(*n*)** with $n \neq 8$; thus, for these polymers the crystalline phase is destabilized and only a layered mesophasic structure, of smectic type, is established[7] (see diffraction patterns in Figure 5). In particular, the diffraction pattern of **P-**

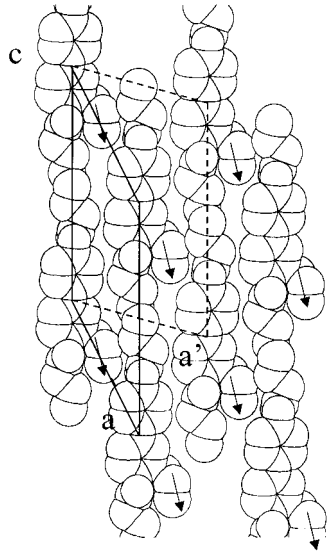

Figure 11. Layered packing of chains along [010]. For the sake of clarity only one of the two statistical allyl units is shown (→).

Table 6. Atomic Fractional Coordinates after Refinement (Standard Deviation in Parentheses)

atom	*x*	*y*	*z*
C1	−0.0093(10)	0.0169(19)	−0.0400(55)
C2	0.1748(55)	0.0898(39)	0.0328(116)
C3	0.1563(73)	0.1236(51)	−0.0473(224)
C4	−0.0463(49)	0.0846(93)	−0.2000(273)
C5	−0.2302(27)	0.0117(122)	−0.2726(216)
C6	−0.2114(27)	−0.0220(87)	−0.1924(108)
O7	−0.0642(69)	0.1175(129)	−0.2778(380)
C8	−0.0895(36)	−0.0165(152)	−0.3300(436)
C9	−0.1754(39)	−0.0071(203)	−0.4461(539)
C10	0.0207(41)	0.0109(142)	−0.3846(623)
C11	−0.0365(81)	0.0553(40)	−0.4917(740)
O12	−0.0365(109)	−0.1469(130)	−0.2748(404)
C13	0.3535(122)	0.2017(80)	0.0307(290)
C14	0.4836(286)	0.0842(126)	0.0602(441)
C15	0.4825(514)	0.1044(334)	−0.0078(595)

(12) (Figure 5b) shows an out-meridian reflection on the first and the third layers, while a stronger meridional reflection appear on the second layer. This pattern is typical of a frustrated smectic A packing. Jung, Hudson, and Lenz[17] have shown that this pattern can be reproduced by chain aggregation in bundles, with rigid moieties tightly packed. For a reason ascribed to the better lateral registry, the bundles are shifted with respect to one other along the *z* direction by *c*/2, giving a two-dimensional rectangular array. Consequently, the even 00*l* reflections are extinguished. The lateral size of each bundle can be evaluated from the equatorial component of the scattering vectors corresponding to the out-meridian reflections. For **P(12)** we found a size of about 18 Å, corresponding to three to four chains in the hypothesis of a tight face-to-face packing in the bundle. Similar to Jung et al.,[17] Nakata and Watanabe[18] reported on a frustrated smectic packing for segmented LC copolymers with different flexible spacers along the chain. In this case, the frustrated structure is observed only when the flexible spacers have an adequate difference in their lengths, thus promoting a bilayer segregation.

About biphenyl, the occurrence of a planar conformation for **P(8)** is not surprising.[19] In fact, the energy barrier around phenyl to phenyl bond is quite low,[20] thus planar conformation is possible if ensuring good molecular packing. Actually, biphenyl is reported to be planar in many crystalline compounds, the molecular structures of which were solved by the single-crystal technique. In the case of 4,4′-dihydroxybiphenyl, the conformation is perfectly planar;[21] in other cases, it is just slightly distorted.[22] Keeping in mind the statistical displacement, allyl units are packed close to each other as shown in Figure 11. We have recently found that **P-(8)** cross-links when UV irradiated in the solid state at room temperature.[8] The short contact between allyl units in the molecular packing is consistent with this finding. Actually, also the analogous homopolymers **P-(*n*)** with $n \neq 8$ cross-link by UV irradiation at room temperature. As already outlined, they are not crystalline but show a layered mesophasic structure of smectic type. Thus, the occurrence of allyl to allyl short contact may be hypothesized even for **P(*n*)** with $n \neq 8$, but in a less ordered fashion.

The screw axis operator generates a second layer of chains in a way that biphenyl units of the two layers interact with an "edge to face" contact (Figures 8 and 9). This corresponds to have a "herringbone" type packing of rigid biphenyl units along [001]. Herringbone packing is only "apparent" because biphenyl units are translated along *c* axis in an amount that the two phenyl rings are involved in the edge to face contact with different adjacent biphenyl units. In the layer, carbonyls do not interact with each other. Qualitatively, this packing arrangement is close to that depicted by Krigbaum et al.[14] Common features are face to edge biphenyl interaction and the large transversal shift of adjacent chains along *z* (large β). Moreover, the similarity with the molecular packing of a low molecular weight compound reported by Centore et al.[22] and having formula

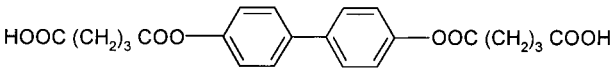

is really interesting. Because of the presence of carboxyl groups, strong hydrogen bonds lead to a polymeric concatenation of small molecules. Polymeric sequences crystallize to a large triclinic cell with six molecules per unit cell. The biphenyl to biphenyl interaction is practically the same as that of **P(8)**, the major difference being the occurrence of two conformations for the biphenyl units: one biphenyl is planar (center of symmetry); the other one has the two phenyl rings slightly staggered with respect to one other (25.0°). In this case, the apparent herringbone packing of "chains" is along [101].

Regarding **P(8−0)**, this polymer shows a spot at low angle in the diffraction pattern that can be indexed as the 100 reflection (see Table 2). Consequently, the glide plane is absent in the molecular packing of **P(8−0)**, with the two chains in the unit cell shifted each other along *z* direction ($z_0 \neq 0$). In other words, the center of mass of the biphenyl unit is not at the origin of the unit cell, and the asymmetric unit corresponds to the whole chain. Thus, the two allyl units attached to the biphenyl affect the biphenyl-to-biphenyl interaction breaking the glide symmetry of the molecular packing.

Conclusion

The molecular packing in the crystalline phase of **P-(8)** is mainly characterized by the layered organization of chains. The transversal intercalation of flexible and rigid units in the layer, due to their almost identical

length, promotes this molecular organization. Repetition of layers in space leads to pseudo-herringbone packing of biphenyl units along [001], as frequently observed for aromatic main-chain polymers, and a pseudohexagonal register of chains along [010].

In the crystalline phase, allyl groups are packed close to each other. This circumstance is in agreement with our recent finding of the extensive cross-linking of allyl groups by UV irradiation in the solid state of **P(*n*)**.[8]

Acknowledgment. Support by Ministero dell'Università e della Ricerca Scientifica e Tecnologica in partially financing this research project is acknowledged (Progetto Nazionale: Sistemi Polimerici per Materiali Compositi).

References and Notes

(1) Leadbetter, A. J. In *Thermotropic Liquid Crystals*; Gray, G. W., Ed.; Wiley & Sons: UK, 1987.
(2) *Liquid Crystals and Plastic Crystals*; Gray, G. W., Winsor, P. A., Eds.; Horwood: Chichester, England, 1974.
(3) *Liquid Crystalline Order in Polymers*; Blumstein, A., Ed.; Academic Press: New York, 1978.
(4) *Polymeric Liquid Crystals*; Blumstein, A., Ed.; Plenum Press: New York, 1985.
(5) Ungar, G. *Polymer* **1993**, *34*, 2050.
(6) Flory, P. J. In *Polymer Liquid Crystals*, Ciferri, A.; Krigbaum, W. R., Meyer, R. B., Eds; Academic Press: New York, 1982, and references therein.
(7) Acierno, D.; Fresa, R.; Iannelli, P.; Vacca, P. *Polymer* **2000**, *41*, 4179.
(8) Acierno, D.; Fresa, R.; Iannelli, P.; Vacca, P. *Polymer* **2000**, *41*, 7785.
(9) Caruso, U.; Iannelli, P.; Roviello, A.; Sirigu, A. *J. Polym. Sci., Polym. Phys.* **1998**, *36*, 2371.
(10) Fu, Y.; Busing, W. R.; Jin, Y.; Affholter, K. A.; Wunderlich, B. *Macromolecules* **1993**, *26*, 2187.
(11) Iannelli, P. *Macromolecules* **1993**, *26*, 2303.
(12) Iannelli, P. *Macromolecules* **1993**, *26*, 2309.
(13) Iannelli, P. *J. Appl. Crystallogr.* **1994**, *27*, 1055.
(14) Krigbaum, W. R.; Watanabe, J.; Ishikawa, T. *Macromolecules* **1983**, *16*, 1271.
(15) Asrar, J.; Toriumi, H.; Watanabe, J.; Krigbaum, W. R.; Ciferri, A. *J. Polym. Sci., Polym. Phys.* **1983**, *21*, 1119.
(16) Stambaugh, B.; Koenig, J. L.; Lando, J. B. *J. Polym. Sci., Phys. Ed.* **1979**, *17*, 1053.
(17) Jung, H.-T.; Hudson, S. D.; Lenz, R. W. *Macromolecules* **1998**, *31*, 637.
(18) Nakata, Y.; Watanabe, J. *Polym. J.* **1997**, *29*, 193.
(19) Brock, C. P. *Acta Crystallogr.* **1980**, *B36*, 968 and references therein.
(20) Lauprête, F.; Noël, C. In *Liquid Crystallinity in Polymers*; Ciferri, X, Ed.; VCH Publishers: New York, 1991.
(21) Trotter, J. *Acta Crystallogr.* **1961**, *14*, 1135.
(22) Centore, R.; Ciajolo, M. R.; Roviello, A.; Sirigu, A.; Tuzi, A. *Mol. Cryst. Liq. Cryst.* **1992**, *214*, 105.

MA0012346